IOSR Journal of Applied Geology and Geophysics (IOSR-JAGG)
e-ISSN: 2321–0990, p-ISSN: 2321–0982.Volume 11, Issue 4 Ser. II (July. – Aug. 2023), 47-58
www.iosrjournals.org

Surface And Subsurface Study At The Area Surrounding Gebel Umm Rabul, Northern Eastern Desert, Egypt Using Airborne Magnetic And Radiometric Data

Asmaa A. Azzazy, Ahmed A. Elhusseiny, Ahmed Tarshan, Mostafa A.M
Nuclear Materials Authority, P.O. Box 530, El Maadi, Cairo, Egypt.

ABSTRACT
This research work aims essentially to detect geologic structure trends affecting the study area, determine radiometric anomalous areas and define alteration zones. Airborne magnetic data were used to detect the geologic structure trends affecting the study area through applying edge detectors such as total horizontal derivative and tilt derivative. The radio-spectrometry data were used in determining the uranium anomalous areas. In addition, radio-spectrometry data were used also to identify the alteration zones by applying F-parameter technique.
The integration between magnetic data and radio-spectrometry illustrates that there is a well correlated relation between surface and subsurface structure, as well as between the alteration zones and radiometric anomalies. These good correlations mean that the radiometric anomalies in the study area is not only a result of natural lithological distribution but also due to the deformation occurred because of the hydrothermal alteration processes and different structural movements, which trending mainly in NE-SW and NW-SE direction.
Keywords: *Structure trends, Uranium zones, Alteration zones, Magnetic analysis*

Date of Submission: 10-08-2023 Date of Acceptance: 20-08-2023

I. INTRODUCTION

The study area is located in the Northern Eastern Desert of Egypt between latitudes 28° 01' 05" & 28° 41' 02" N and longitudes 32° 14' 09" & 33° 12' 55" E, covering an area of about 5447 Km^2 (Fig. 1a). The topographic map shows that the north western corner of the area reaches an elevation of 1680 m while it reaches 1600 m at G. Ghuweirib at the south of the area. Elevations on the eastern side decrease to 10 meters (Fig. 1b).

Eastern Desert of Egypt has been considered the main target for mineral resources exploration, which was hosted by Precambrian rocks. There are many researches that concern with mineralization mapping, especially radioactive minerals (e.g. Abdel Hafeez et al., 2015; Minty and FitzGerald, 2015; Ahmed, 2018). Radioactive anomaly zones are the result of two main reasons; natural lithological distribution and post magmatic processes caused by either hydrothermal solutions and/or dikes factors. Therefore, mineralization zones investigation is mainly done by evaluating lithological units, alteration, and structural features (e.g.: Bishta, 2013; Pour et al., 2018; Chattoraj et al., 2020). This study aims essentially to deduce the radioactive mineralization zones, the hydrothermal alteration areas and the structure controlling the mineralization.

Airborne magnetic data are usually used in mapping the shallow and deep geologic structures and enlightening intrusions (Holden et al., 2011). These structures are represented in trends and intensities on magnetic maps that represent magnetic patterns (Gay, 1972). The spectrometric maps of the study area will help to locate the high alteration areas of the radioactive minerals and discriminate the boundaries of the different rocks. In addition, the spectrometric data will be used as a guide for alteration zones.

II. GEOLOGIC SETTING

The Eastern Desert of Egypt is separated into Northern, Central, and Southern parts depending on the basement characteristics (Stern and Hedge, 1985). The area represents part of the Northern Eastern Desert of Egypt. The study area consists of basement rocks at the middle which trending NW-SE direction (Fig. 2). These rocks are intersected by numerous wadis filled with Quaternary sediments.

These rocks could be seen on geological map (Fig. 2) such as Metagabbro, Acidic Metavolcanics, Older Granite (felsic plutonic rocks of essentially intermediate composition), Younger Granite (mostly occurs as isolated, equidimensional plutons of 1 to 10 km diameter) and Dokhan Volcanics (Dardir and Abu Zeid, 1972; Essawy and Abu Zeid, 1972). The sedimentary cover which occupies both sides of basement rocks extend in age from Cambrian to Quaternary. The Cambrian age is represented by Araba formation while Samr El-Qa formation is representing the lower Carboniferous age. The Upper Cretaceous rocks are represented by Malha, Wadi Qena, Galala, Umm Omeiyid, Hawashiya, Rakhiyat and Sudr formations while the Tertiary rock units are represented by Esna, Abu Rimth, Thebes, Mokattam, Um Mahara, Um Gheig, Miocene and Shagra formations and Pliocene deposits (Said, 1962). Quaternary and Wadi deposits are mainly pebbles of sand, detritus, cobbles and little boulders filling the main wadis. The geologic map (Fig. 2) shows that the area is affected by many normal faults; majority of these faults are trending in NE-SW direction and in lesser extent in NW-SE direction.

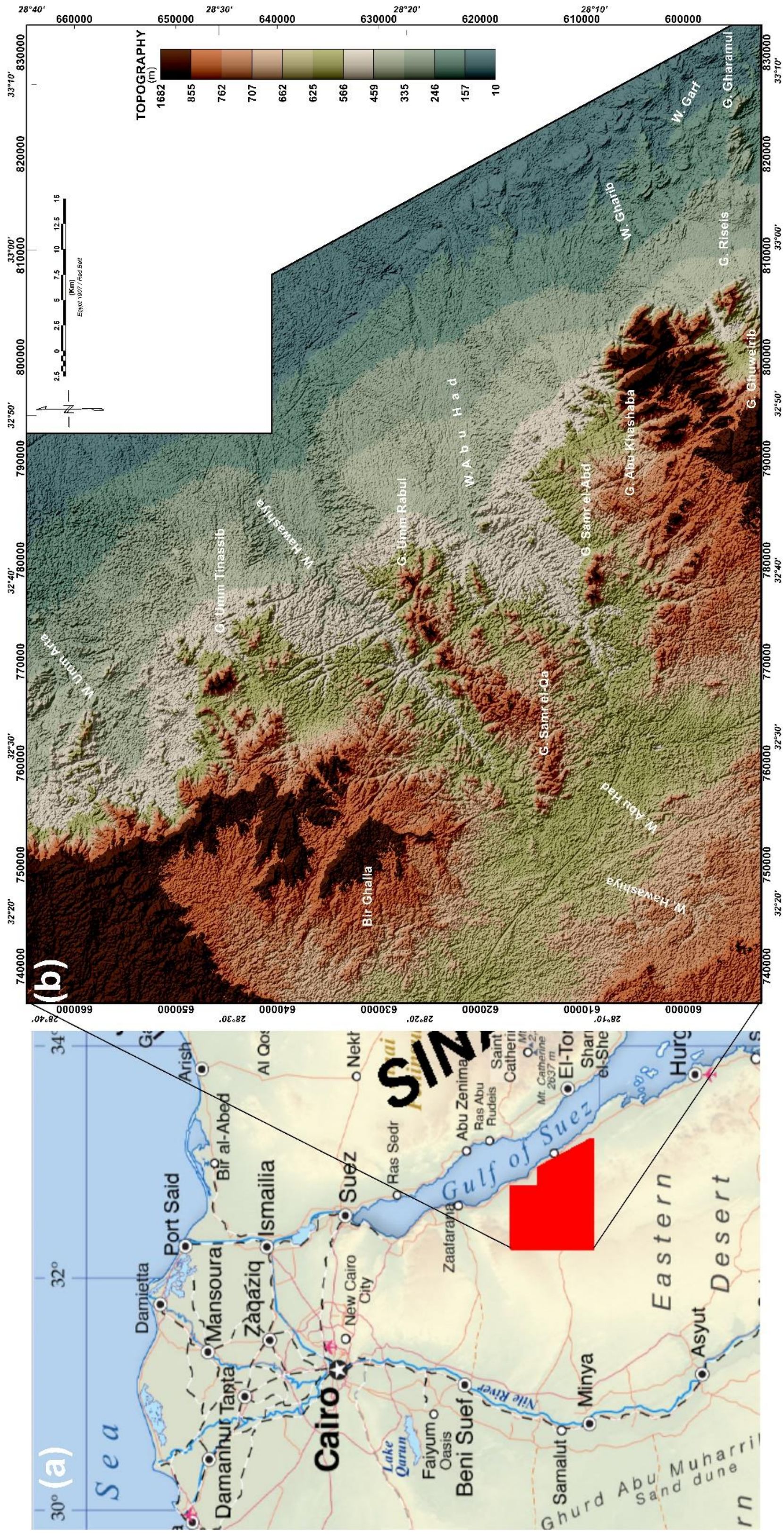

Figure. 1: (a) Location map of the study area, (b) Topographic map of the study area

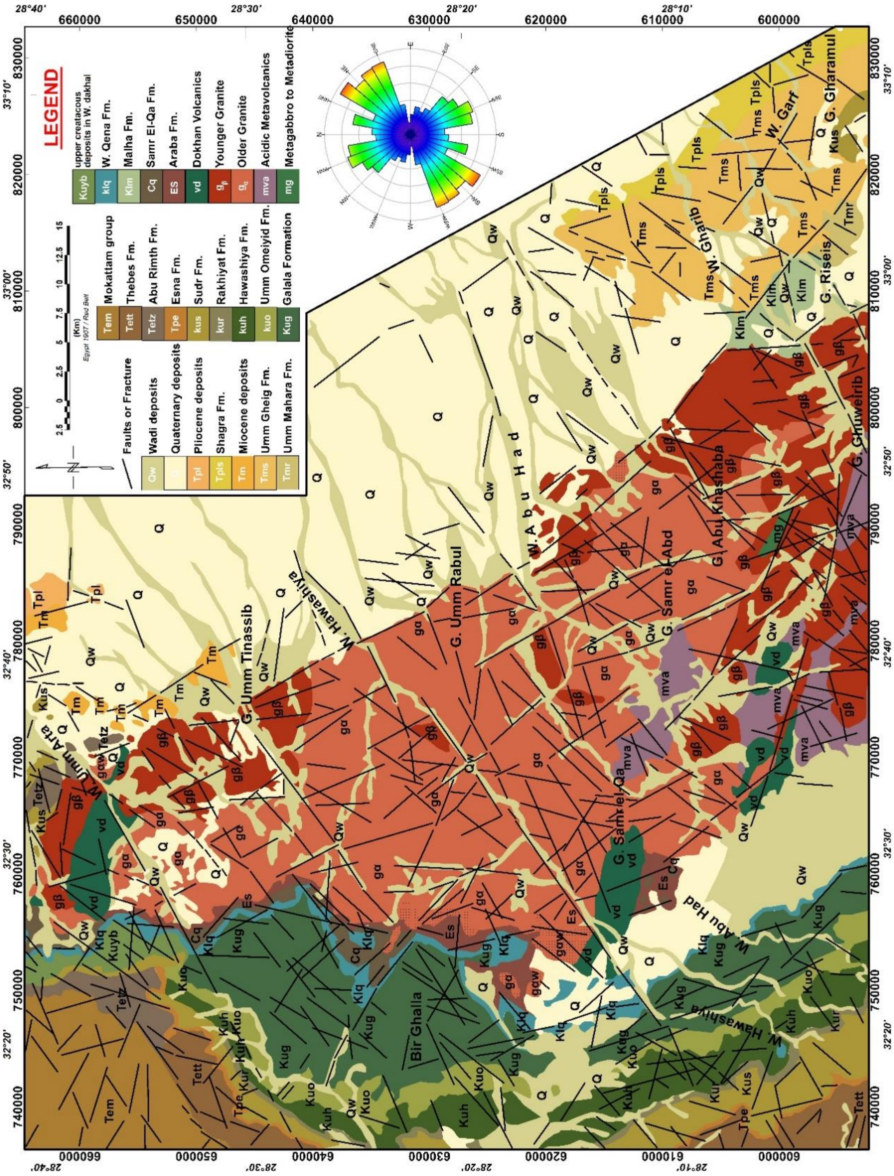

Figure. 2: Geologic map of the study area, after conco,1987

III. DATA AND METHODOLOGY

In this research work airborne magnetic and radio-spectrometric survey data were used. The magnetic and spectrometry data were acquired along flight lines extending in NE-SW direction with 1.5 km spacing, while the tie lines were flown along profiles perpendicular to the flight lines (NW-SE) with 10 km spacing. The nominal flying altitude was 120 m above ground level (Aeroservice, 1984).

Magnetic Data

The final total magnetic intensity (TMI) data was gridded with suitable grid cell size and presented in figure (3). The TMI data were reduced to the north magnetic pole (RTP) to overcome the distortion in shape and location produced by the dipolarity problem (Ibraheem et al., 2018) and presented in figure (4). The RTP map shows clearly the signature of positive anomalies over the basement rocks which trending in NW-SE direction and have magnetic intensity reaches 159 nT. Another positive anomaly was noticed at the south eastern part of the study area over Quaternary sediments.

The magnetic data were used in this work to detect the geological structures which controlling the mineralization process present in the area. To achieve this goal, two techniques for detecting edges of magnetic source have been introduced: total horizontal derivative (Cordell and Grauch, 1985) and tilt angle derivative (Cooper and Cowan, 2006). Total horizontal derivative (THD) depends on the fact that the amplitude of the horizontal derivative of the RTP magnetic field resulted from a tabular body has the highest values over the anomaly edges in case of vertical edges and well-separated edges from each other (Cordell and Grauch, 1985).

The method can be used to delineate trends of subsurface faults (Grant and West 1965). It is less sensitive to noise and very strong in detection magnetic sources at shallow depths (Phillips, 2002).

In noisy data, tilt derivative (TD) technique is very powerful edge detector and responds equally well for both shallow- and deep-seated magnetic sources because it elaborates like an automatic gain-control filter (Arisoy and Dikmen, 2013). Due to the nature of the arctangent trigonometric function, TD amplitude has a range of $-\pi/2$ and $+\pi/2$. Moreover, the amplitude of the TD has three rates: positive over the magnetic body, zero at/close to the body's edges, and negative elsewhere (Miller and Singh, 1994; Ibraheem et al 2019). The two techniques (THD & TD) were used to figure out the trends affecting the study area and, consequently, the mineralization process. These techniques and their result were presented in figure (5).

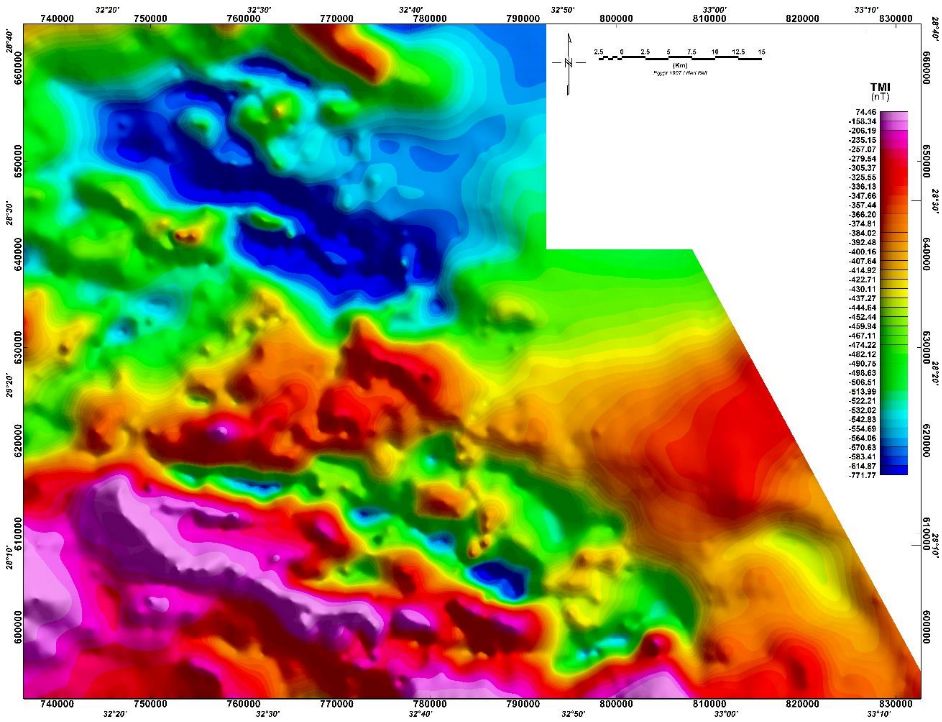

Figure. 3: Total magnetic intensity (TMI) map of the study area

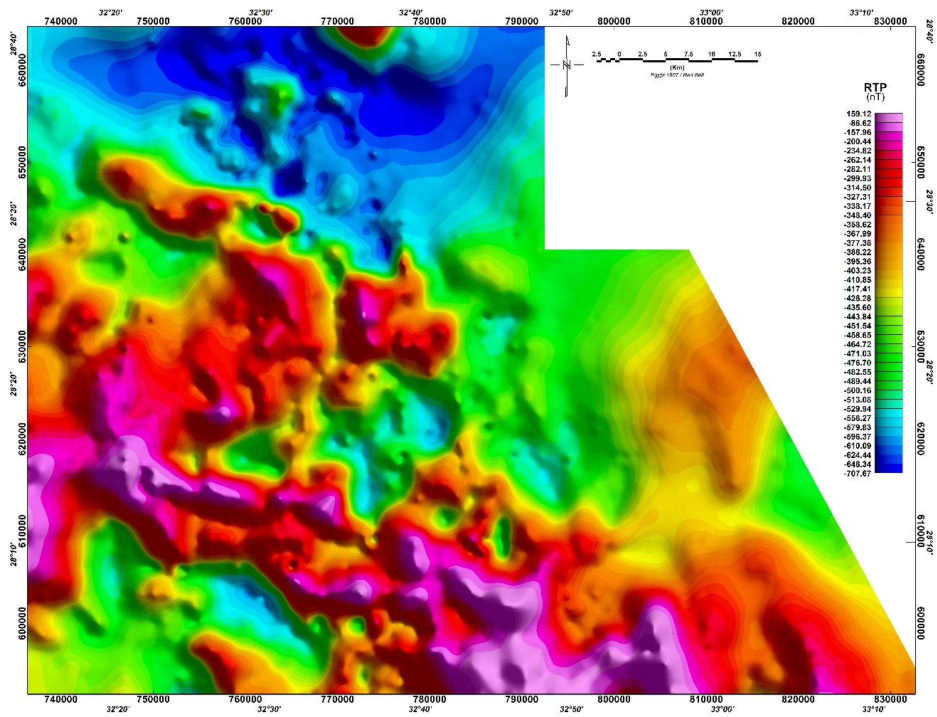

Figure. 4: Reduced to the North magnetic pole (RTP) map of the study area

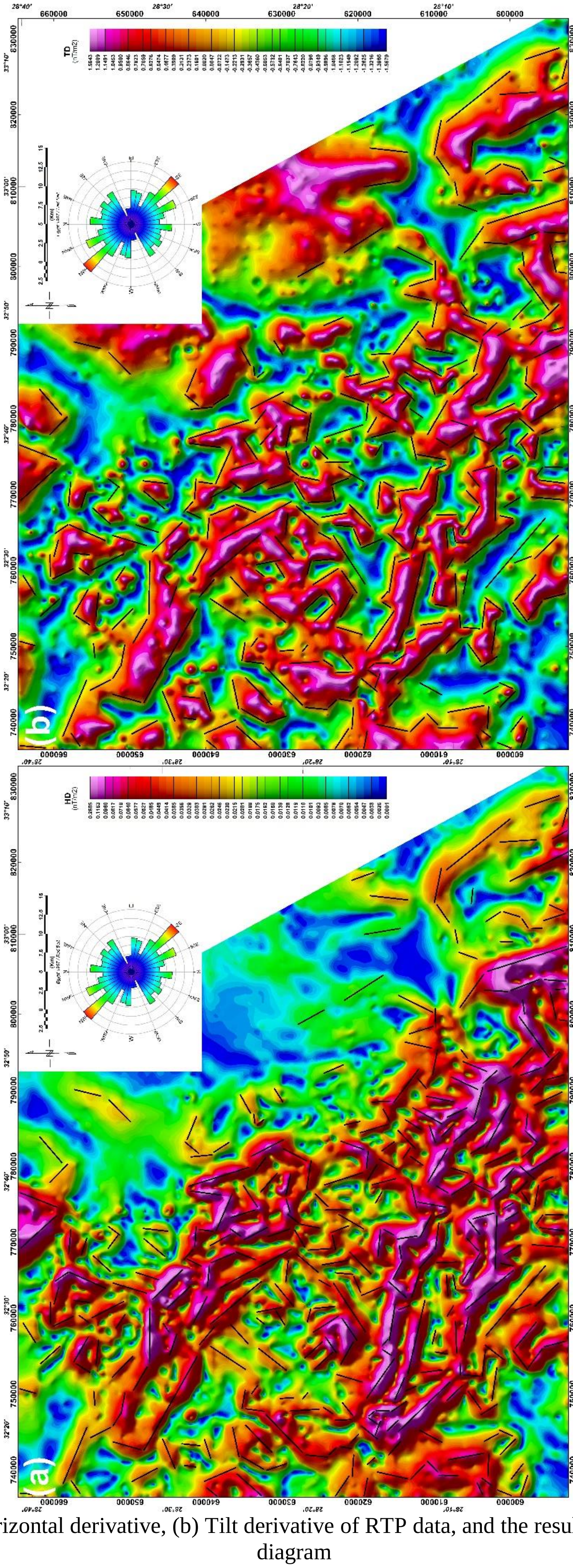

Figure. 5: (a) Total horizontal derivative, (b) Tilt derivative of RTP data, and the resulted lineation and its rose diagram

Radio-spectrometric Data

The qualitative interpretation of the airborne gamma-ray spectrometric data depends mainly upon the excellent correlation between the general pattern of the recorded measurements and the surface distribution of rock units. The texture of the radio-spectrometric contour lines (signatures) could be an aid during interpretation of surface geology (lithology and structure) (IAEA, 1979).

The main windows of radio-spectrometric data were gridded and presented in figures (6 to 9). Total Count map (TC) (Fig. 6) has values from 0.0 to 211 µR/h. The highest values are related mainly to younger granites (gβ) which located at the north and south eastern parts (basement rocks trend), and in lesser extent with parts of Dokhan volcanics (vd) and older granites (gα). The highest values which occur over the Quaternary sediments (Q) may be due to the migration process.

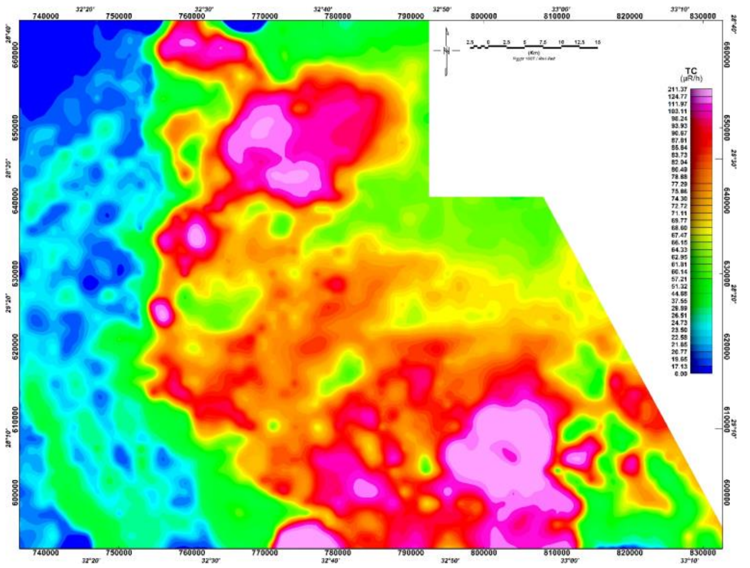

Figure. 6: Total count (TC) map of the study area

The distribution of Potassium concentrations in the study area (Fig. 7) resemble to great extent the distribution of TC concentrations. Equivalent uranium concentrations range from 1.2 to 36 ppm (Fig. 8). The highest values related mainly with younger granites (gβ) and small parts of Dokhan volcanics (vd) and older granites (gα) as in TC map (Fig. 6). Another high anomaly is found over Rakhyiat formation (Kur) as it consists of marine shale with phosphate beds. Equivalent thorium map is also presented in figure (9) with values reach about 120 ppm. As the aforementioned maps (Figs. 6 to 8), the distribution of high values of equivalent thorium is also related mainly to the younger granitic rocks of the study area.

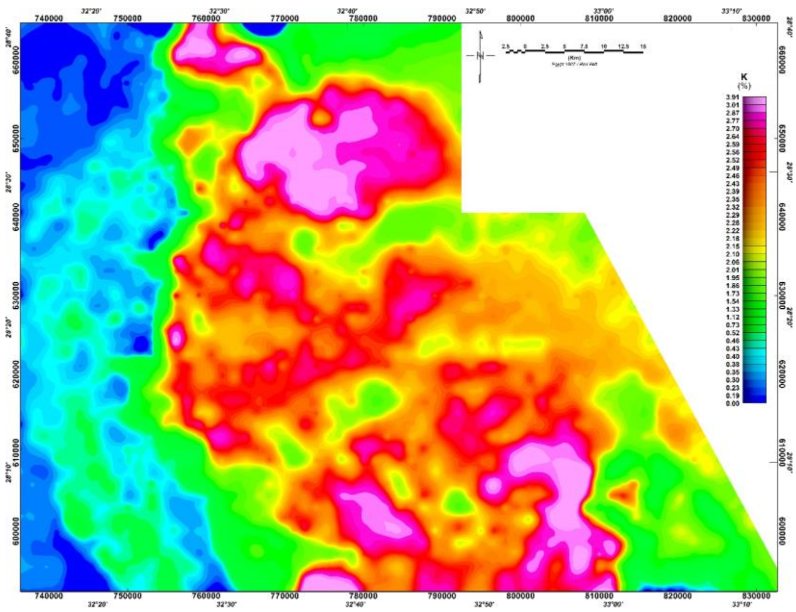

Figure. 7: Potassium (K) map of the study area

Every rock unit has different content of potassium, uranium, and thorium. Therefore, these contents can be used to detect lithology and contacts between constraining lithologies (Elkhadragy. et al, 2016). The radioelements composite image (Fig. 10) of the study area shows the variations occurring in the three radioelements concentrations, which mainly reflect lithologic variations. It was noticed that the higher bright zones (means high in the three elements) are clearly correlated with younger granite rocks. Meanwhile, the ternary composite image shows dark areas of weak radioelement contents as indicative to the low radioactive rocks. The other remarkable notice is that the green colour which represents 100% of uranium concentration is well coincident with Rakhyiat formation (Kur) at the western part of the study area.

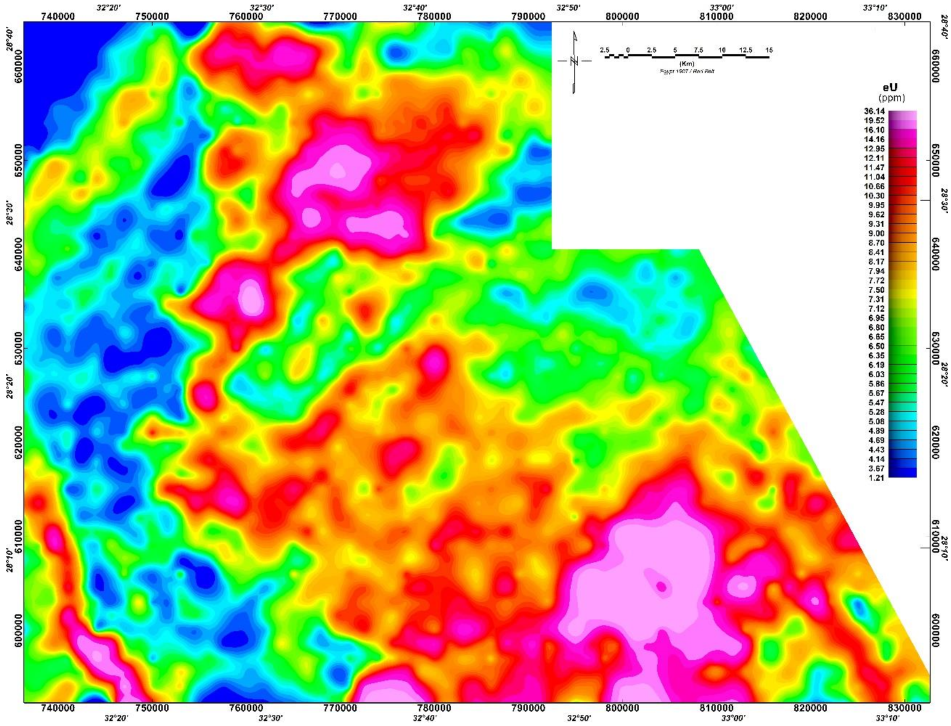

Figure. 8: Equivalent uranium (eU) map of the study area

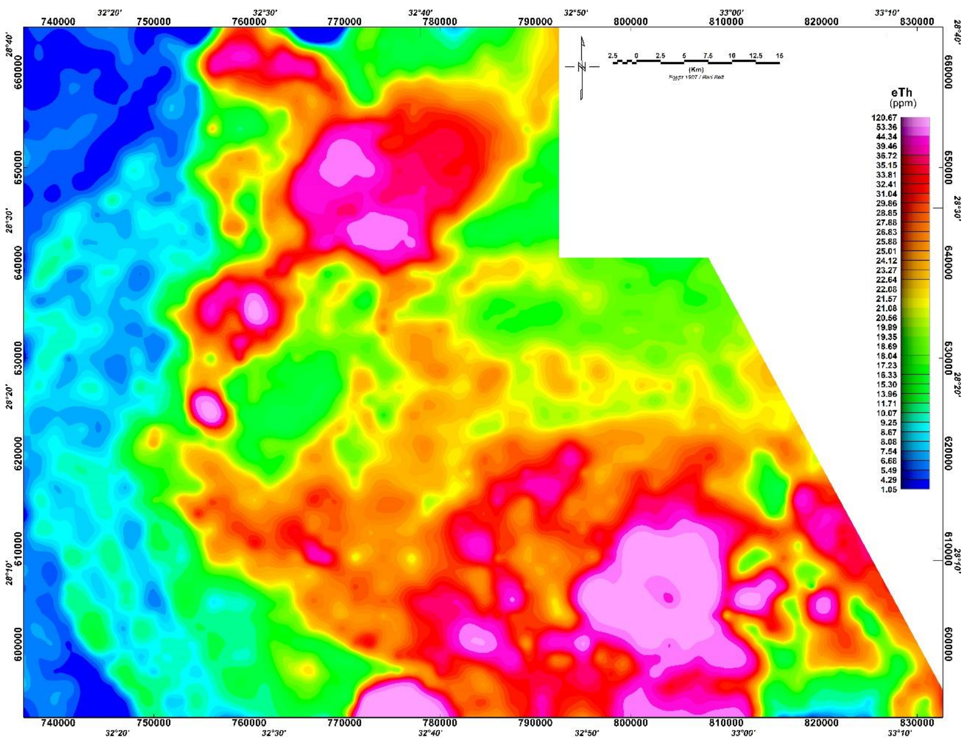

Figure. 9: Equivalent thorium (eTh) map of the study area

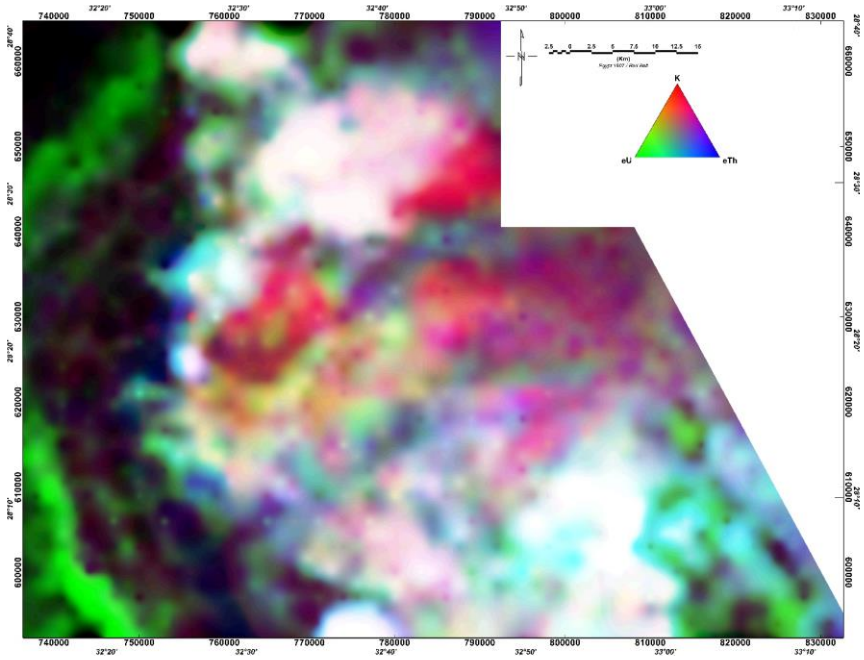

Figure. 10: Radioelement composite image of the study area

To identify the locations of anomalies, some statistical analyses were calculated for each of potassium, equivalent uranium, and equivalent thorium, such as the arithmetic mean (M) and standard deviation (S). According to the Saunders and Potts rule in 1978, the values of (M+S), (M+2S), and (M+3S) were calculated and used to detect these anomalies (Table. 1).

Table. 1: Statistical analysis of radiometric windows

Window	Min	Max	M	S	M+S	M+2S	M+3S
K	0	3.79	1.73	0.96	2.69	3.65	4.61
eU	1.35	36.27	8.74	4.28	13.02	17.3	21.58
eTh	0	114.22	22.32	13.43	35.75	49.18	62.61

In addition, the hydrothermal alteration zones which may be related to the radiometric minerals and in hence with the accompanied minerals can be detected using F-parameter technique which was proposed by Efimov in 1978 (stated in Gnojek et al., 1985). This F-parameter seems to be very useful, because it comprises two important characteristics of the rock environment, i.e., the potassium abundance to the Th/U ratio and the uranium abundance to the Th/K ratio, as expressed in the relation:

$F = \frac{K*U}{Th} = \frac{K}{Th/U} = \frac{U}{Th/K}$……………………………(1)

Efimov (1978) who only quantified the F-parameter showed that it can acquire values up to 1.2 or 1.3 in common non-altered rocks, while in altered rocks it may attains 2 or 5, exceptionally 10 (quoted from Gnojek et al., 1985). The use of this method for geological and mineral exploration assumes that different rock types or ore-bearing rock types are composed of certain amounts of rock forming minerals which comprise specific quantities of radioactive elements such as potassium, uranium, and thorium. To be able to evaluate the results of the gamma-ray spectrometric survey, it will be necessary to know roughly the behavior of the different radioactive elements through a complete geological cycle (Cambon et al., 1997). The F-parameter map is displayed in figure (11) and showed that the highest values which reaches 1.5 are related mainly with younger granites and parts of Dokhan volcanics and older granites.

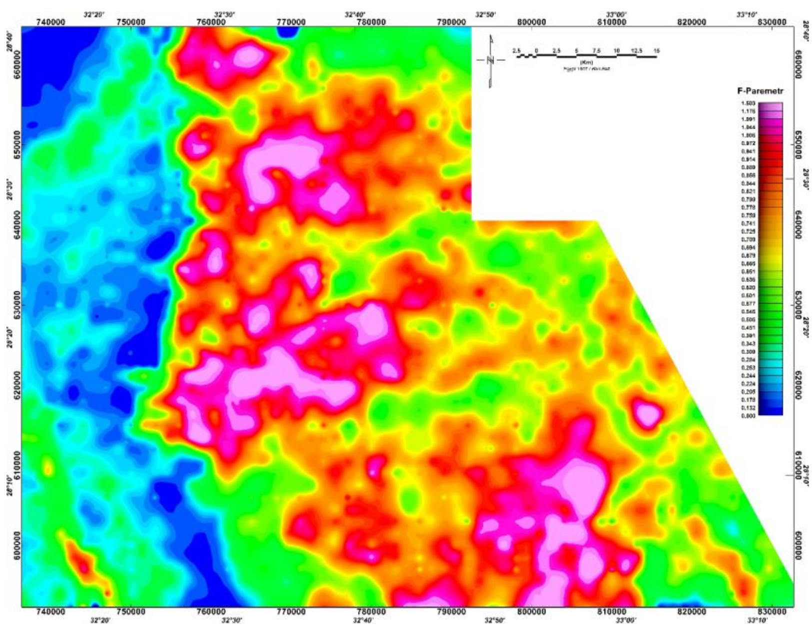

Figure. 11: F-parameter map of the study area

In addition, after the calculations of potassium, equivalent uranium, and equivalent thorium anomalies and deducing the parts which submitted to hydrothermal alteration processes from the F-parameter map; a new map was produced to illustrate the relation between the alteration zones and radiometric anomalies (Fig. 12). This map showed that the majority of the radiometric anomalies were well correlated with the areas of hydrothermal alterations. On the other hand, there are parts related to the older granites which have alterations process but not related to any anomalies, whereas there are some anomalies which related to the sedimentary cover (Rakhyiat formation) which have no alteration processes.

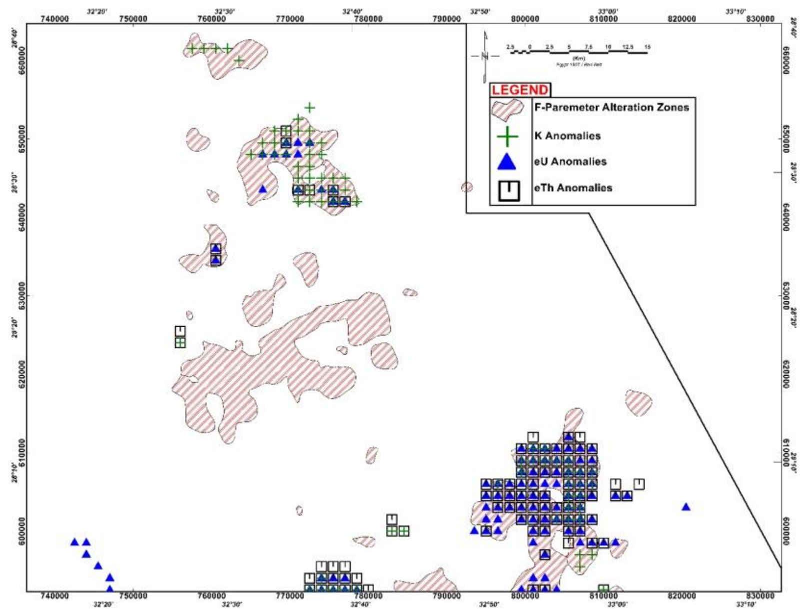

Figure. 12: Key map showing the alteration zones and radiometric anomalies

IV. RESULTS AND DISCUSSION

The main aim of this research work is to deduce radioactive mineralization, determine the alteration zones which related to mineralization accumulation and geologic structure trends affecting the study area. The integration between geophysical data is a good tool for delineating and interpreting the objectives of the study.

The different geological structures that affect the study area are of the most important factors that affect the mineralization accumulation. Magnetic method is very valuable tool to delineate the subsurface structure and basement configuration. In this work, the subsurface structure trends (deep and shallow trends) were delineated through magnetic method by using the edge detectors (THD and TD) and presented in figure (5). In addition to the subsurface trends, surface trends were traced from the geological map (Fig. 2). The two different set of lineaments (Figs. 2 & 5) illustrated the presence of NW-SE trend. In the subsurface results, this trend is the predominant trend whereas the surface lineaments exhibit NE-SW trend as the main trend with the presence of NW-SE trend as the second order trend.

To link the results of different geologic structure (surface and subsurface) with the anomalies of potassium, equivalent uranium, and equivalent thorium and also with the hydrothermal alteration zones, these sets of lineaments were submitted to line density technique. The line density technique was resulted using the ArcMap line density tool; it shows the frequency of lineaments per unit area. The line density maps show that the higher densities reflect the topographic variation for the exposed lithological units, thus it indicates that the basement and sedimentary rocks in this area are highly deformed. The density technique was applied to surface geologic lineaments and subsurface magnetic lineaments, overlaid by the alteration zones and radiometric anomalies in integrated maps displayed in figures (13 & 14) respectively.

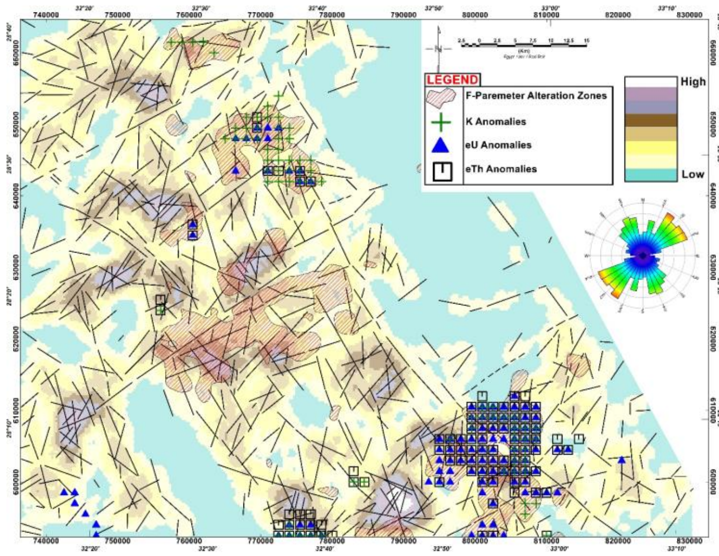

Figure. 13: Key map showing the line density of surface geologic lineaments overlaid by the alteration zones and radiometric anomalies

Figure (13) shows clearly that most of alteration zones, which related to younger granite rocks and parts of older granite rocks and Dokhan volcanics, were well correlated to the areas of high density of lineaments. This result clearly led to the fact that the deformation of these rock units is also related to the structures. The radiometric anomalies are also related to this high density of lineaments. The majority of these lineaments which affected the mineralization is mainly in two directions displayed clearly on the map (Fig. 13); NE-SW and NW-SE.

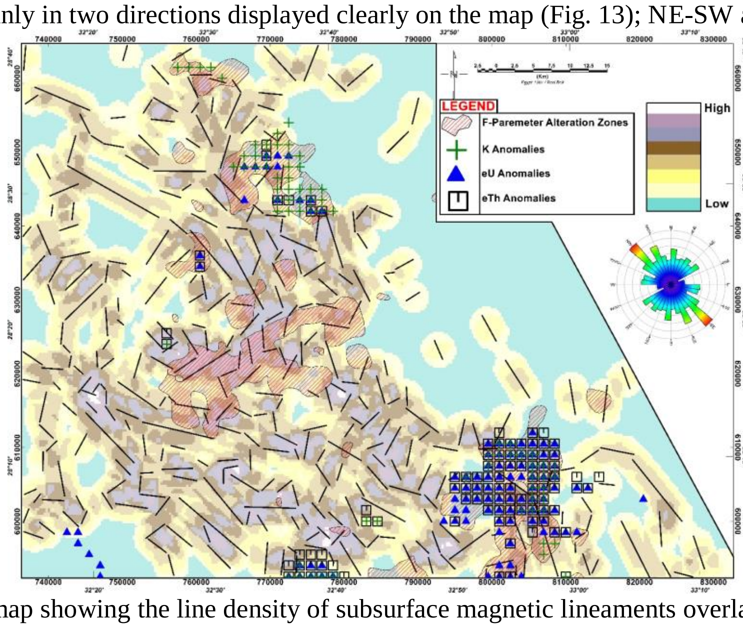

Figure. 14: Key map showing the line density of subsurface magnetic lineaments overlaid by the alteration zones and radiometric anomalies

In a manner similar to figure (13), Figure (14) also emphasizes the well correlation between the radiometric anomalies and alteration zones on the one hand and the density of magnetic lineaments on the other hand. This correlation means that the radiometric anomalies are not only due to natural lithological distribution but also post magmatic processes may be caused by hydrothermal solutions and geologic structures.

V. CONCLUSION

The research aims essentially to deduce the relation between the surface and subsurface structures, as well as the relation between the alteration zones and radiometric anomalies. Many techniques were used to clarify the structure trends which affect the study area such as total horizontal derivative, tilt derivative, and line density tool.

The radiometric anomalies deduced from spectrometric data are well correlated with hydrothermal alteration zones deduced from F-parameter technique. These anomalies are recorded mainly over younger granite rocks and, in lesser extent, over parts of Dokhan volcanics and older granite rocks.

The integration between magnetic and spectrometric data was introduced through producing maps consisting of the results of the two sets of data. This integration led to the fact that most of radiometric anomalies and alteration zones are well correlated with the highest densities of surface and subsurface structure lineaments. In other way, the anomalies are not only due to natural lithological distribution but also structurally controlled.

REFRENCES

[1]. Abdel Hafeez, Th. H., Youssef, M. A. S. And Mohamed, W. H., 2015: Engineering Utilization Of Airborne Gamma Ray Spectrometric Data For Geological Mapping And Radioactive Mineral Exploration Of Gabel Umm Tineidba Area, Southeastern Desert, Egypt. World Journal Of Engineering 12, 149-160.

[2]. Ahmed, S. B., 2018: Integration Of Airborne Geophysical And Satellite Imagery Data To Delineate The Radioactive Zones At West Safaga Area, Eastern Desert, Egypt. NRIAG Journal Of Astronomy And Geophysics, 7, 297- 308.

[3]. Aeroservice, (1984): Final Operational Report Of Airborne Magnetic/Radiation Survey In The Eastern Desert, Egypt, For The Egyptian General Petroleum Corporation: Aeroservice Division, Houston, Texas, 1984, Six Volumes. Western Geophysical Company Of America.

[4]. Arisoy, M. And Dikmen, Ü., 2013: Edge Detection Of Magnetic Sources Using Enhanced Total Horizontal Derivative Of The Tilt Angle. Bulletin Of The Earth Sciences Application And Research Centre Of Hacettepe University, 34, 1, 73–82.

[5]. Bishta, A. Z., 2013: Utilities Of Landsat 7 Data And Selective Image Processing In Characterization Of Radioactivity Zones Ofwadi Baba–Wadi Shalal Area, Westcentral Sinai, Egypt. Arab J Geosci, 6, 3513-3526.

[6]. Cambon, R., 1997: Spectrometric Aerial Survey As A New Tool For Geological Survey And Mining Prospecting. In "Uranium Exploratin Data And Techniques Applied To The Preparation Of Radioelement Maps", International Atomic Energy Agency (IAEA), Vienna, Austria, Pp. 403-407.

[7]. Conoco., 1987: Geological Map Of Egypt, Scale 1: 500,000. The Egyptian General Petroleum Corporation (EGPC), Cairo, Egypt.

[8]. Cooper, G.R.J And Cowan, D.R. 2006: Enhancing Potential Field Data Using Filters Based On The Local Phase. Comput. Geosci. 32, 1585–1591.

[9]. Cordell, L. And Grauch, V.J.S., 1985: Mapping Basement Magnetization Zones From Aeromagnetic Data In The San Juan Basin, New Mexico. In: Hinzc, W.J., Ed. The Utility Of Regional Gravity And Magnetic Anomaly Maps; Society Of Exploration Geophysicists: Tulsa, OK, USA, 181–197.

[10]. Chattoraj, S. L., Prasad, G., Sharma, R. U., Champati Ray, P. K., Van Der Meer, F. D., Guha, A., Pour, A. B., 2020: Integration Of Remote Sensing, Gravity, And Geochemical Data For Exploration Of Cu-Mineralization In Alwar Basin, Rajasthan, India. International Journal Of Applied Earth Observation And Geoinformation, 91, Https://Doi.Org/10.1016/J.Jag.2020.102162.

[11]. Dardir, A. A. And Abu Zeid, K. M., 1972: Geology Of The Basement Rocks Between Latitudes 27 00 And 27 30 N, Eastern Desert, Ann. Geol. Surv, Egypt, 2, 129–159.

[12]. Efimov, A. V., 1978: Multiplikatinnyi Pokazatel Dlja Vydelenija Endogennych Rud Po Aerogamma-Spektrometriceskim Dannym. In "Metody Rudnoj Geofiziki", Geofizika, Leningrad, USSR.

[13]. Elkhadragy, A.A. & Ismail, A.A. & Eltarras, M.M. & Azzazy, Asmaa., 2016: Utilization Of Airborne Gamma Ray Spectrometric Data For Radioactive Mineral Exploration Of G.Abu Had – G.Umm Qaraf Area, South Eastern Desert, Egypt. NRIAG Journal Of Astronomy And Geophysics. 6. 10.1016/J.Nrjag.2016.12.001.

[14]. Essawy, M. A. And Abu Zeid, K. M., 1972: Atalla Felsite Intrusion And Its Neighboring Flows And Tuffs, Eastern Desert, Ann. Geol. Surv. Egypt, 2, 271–280.

[15]. Gay Jr., S.P., 1972: Fundamental Characteristics Of Aeromagnetic Lineaments, Their Geological Significance, And Their Significance To Geology._The New Basement Tectonics' American Stereo Map Company, Sult Lake City, Utah, 94pp.

[16]. Gnojeck, I., Prichystal, A., 1985: A New Zinc Mineralization Detected By Airborne Gamma-Ray Spectrometry In Northern Moravia, Czechoslovakia. Geoexploration, Vol.23, Pp. 491-502.

[17]. Grant, F.S., And West, G.F., 1965: Interpretation Theory In Applied Geophysics, New York: Mcgraw-Hill.

[18]. Holden, E.J., Fu, S.C., Kovesi, P., Dentith, M., Bourne, B., Hope, M., 2011: Automatic Identification Of Responses From Porphyry Intrusive Systems Within Magnetic Data Using Image Analysis. J. Appl. Geophys. 74, 255-262.

[19]. Ibraheem, I.M., Gurk, M., Tougiannidis, N. And Tezkan, B., 2018: Subsurface Imaging Of The Neogene Mygdonian Basin, Greece Using Magnetic Data. Journal Of Pure And Applied Geophysics, 175, 8, 2955–2973.

[20]. Ibraheem, I.M., Haggag, M. And Tezkan, B., 2019: Edge Detectors As Structural Imaging Tools Using Aeromagnetic Data: A Case Study Of Sohag Area, Egypt. Geosciences, 9, 5, 211.Https://Doi.Org/10.3390/Geosciences9050211.

[21]. International Atomic Energy Agency (IAEA), 1979: Gamma-Ray Surveys In Uranium Exploration. Technical Report Series 186, Vienna.

[22]. Miller, H.G. And Singh, V., 1994: Potential Field Tilt—A New Concept For Location Of Potential Field Sources. Journal Of Applied Geophysics, 32, 213–217.

[23]. Minty, B., And Fitzgerald, D., 2015: Developments In Airborne Gamma-Ray Spectrometry To Aid The Search For Strategic Minerals. KEGS Symposium 2015 ''Exploration For Strategic Minerals'' Toronto, Canada, February 28, 2015.

[24]. Phillips, J.D., 2002: Processing And Interpretation Of Aeromagnetic Data For The Santa Cruz Basin-Patahonia Mountains Area, South-Central Arizona; U.S. Geological Survey Open-File Report 02–98; U.S. Geological Survey: Reston, VA, USA.

[25]. Pour, A. B., Park, Y., Park, T. Y.S., Hong, J. K., Hashim, M., Woo, J., Ayoobi, I., 2018: Regional Geology Mapping Using Satellite-Based Remote Sensing Approach In Northern Victoria Land, Antarctica. Polar Sciences, 16, 23-46.

[26]. Said, R., 1962: Geology Of Egypt. Elsevier Publ. Co., Amsterdam And New York, 293–319.

[27]. Saunders, D. F. And Potts, M. J., 1978: Manual For The Application Of NURE 1974-1977 Aerial Gamma-Ray Spectrometer Data. U.S. Dept. Of Energy, Grand Junction Office, Report No. GJBX-13(78).

[28]. Stern R. T., And Hedge C. E., 1985: Geochronologic And Isotopic Constrains On Late Precambrian Crustal Evaluation In The Eastern Desert Of Egypt: Am. Jol. Sci. 285, 97-127.